Fabricating nanowire devices on diverse substrates by simple transfer-printing methods

Chi Hwan Lee, Dong Rip Kim, and Xiaolin Zheng[1]

Department of Mechanical Engineering, Stanford University, CA 94305

Edited* by Charles Lieber, Harvard University, Cambridge, MA, and approved April 19, 2010 (received for review December 4, 2009)

The fabrication of nanowire (NW) devices on diverse substrates is necessary for applications such as flexible electronics, conformable sensors, and transparent solar cells. Although NWs have been fabricated on plastic and glass by lithographic methods, the choice of device substrates is severely limited by the lithographic process temperature and substrate properties. Here we report three new transfer-printing methods for fabricating NW devices on diverse substrates including polydimethylsiloxane, Petri dishes, Kapton tapes, thermal release tapes, and many types of adhesive tapes. These transfer-printing methods rely on the differences in adhesion to transfer NWs, metal films, and devices from weakly adhesive donor substrates to more strongly adhesive receiver substrates. Electrical characterization of fabricated NW devices shows that reliable ohmic contacts are formed between NWs and electrodes. Moreover, we demonstrated that Si NW devices fabricated by the transfer-printing methods are robust piezoresistive stress sensors and temperature sensors with reliable performance.

Semiconductor nanowires (NWs), because of their unique physical and chemical properties, have great potential for applications in the areas of electronics (1–3), photonics (4–7), and bio/chemical sensors (8–13), and the current state of the art of NW devices has been reviewed in refs. 14 and 15. In particular, when semiconductor NW devices are fabricated on flexible substrates, they function as versatile building blocks for high performance flexible and/or transparent electronics (16, 17) with possible extension to flexible displays, touch screens, flexible solar cells, and conformable sensors (8, 16, 17). To realize these NW-based applications, great efforts have been devoted to the fabrication of NW devices on flexible/transparent substrates with methods including conventional photo- and electron beam lithography (6–8, 17). Although NW devices have been successfully fabricated on plastics, glass, and Kapton (6–8, 17, 18), the choice of device substrates is generally restricted because many useful flexible/transparent substrates, such as polydimethylsiloxane (PDMS) and tapes, suffer from problems such as shrinkage or degradation at the processing temperature, poor adhesion to NWs and metal electrodes, incompatibility with solvents and acids, and being too flexible to be handled for the lithography step.

Here we report three simple transfer-printing methods to fabricate NW devices on diverse substrates including PDMS, Petri dishes, Kapton tapes, thermal release tapes, and many types of adhesive tapes. The three transfer-printing methods basically rely on the differences in adhesion to transfer NWs, metal films, and even entire NW devices from weakly adhesive donor substrates to more strongly adhesive receiver substrates when these two substrates are brought into close physical contact. Previously reported transfer-printing methods, such as microcontact printing, nanoscale-transfer printing, and metal transfer printing (16, 19–23), have been used mainly to transfer metal films to receiver substrates by using PDMS stamps. Our methods significantly broaden the transferred substances from metals to the entire NW devices with not only PDMS but also tapes. Significantly, NW devices can be fabricated by printing NWs and metal electrodes in sequence on a diverse range of substrates, including PDMS, tapes, wafers, Kapton, and even Petri dishes.

For convenience, we categorize our transfer-printing techniques into three methods. The first method, referred to as *single transfer printing* (STP), allows existing NW devices to be transferred from a Si wafer to a receiving PDMS or tape substrate by a single peel-off step. In the second method, named *double transfer printing* (DTP), NW devices are fabricated on adhesive substrates by transferring and printing NWs and electrodes in sequence. The third and last method, i.e., *multiple transfer printing* (MTP), involves multiple transfers of electrodes by using thermal release tapes and is capable of fabricating NW devices on both flexible and rigid substrates. The procedures and features of these three methods are discussed below, in detail.

Results and Discussion

STP Method for Fabricating NW Devices. The STP method enables fabrication of NW devices on adhesive substrates, such as PDMS and many types of adhesive tapes, by peeling off prefabricated NW devices from a donor Si wafer by using the adhesive receiver substrates. The STP method was first demonstrated with PDMS as the receiver substrate because PDMS is commonly used for microfluidic and biological applications because of its simplicity in fabrication, excellent elasticity, and biocompatibility (24). The basic steps of transferring NW devices onto PDMS by using the STP method are summarized in Fig. 1*A*. First, aligned Si NWs were deposited on a Si wafer from their growth substrate by the contact-printing method (25). The source and drain contacts (100 nm Au/5 nm Ti) were deposited by electron beam evaporator at photolithography-defined regions to complete the NW devices (Fig. 1*A*(*i*) (9) (see *Materials and Methods*). Next, liquid PDMS was poured onto the prefabricated NW devices and cured overnight at room temperature (Fig. 1*A*(*ii*). Because liquid PDMS has low viscosity and low surface energy, it can easily fill the gaps between NWs and electrodes to fully encapsulate the NW devices (26). Finally, the cured PDMS film (~5 mm) was peeled off from the donor Si wafer with NW devices embedded inside (Fig. 1*A* (*iii*) and (*iv*). Moreover, the procedures described in Fig. 1*A* were also used to fabricate NW devices on adhesive tapes (e.g., thermal release tapes and blue wafer mount tapes) by simply using tapes instead of PDMS.

The NW devices transferred by the STP method exhibit several important features. First, NW devices with electrode spacing ranging from 3 to 25 μm were successfully transferred from the donor Si wafer to PDMS and thermal release tapes (Fig. 1*B*). Optical pictures and SEM inspections show that about 90–100% of the metal electrodes (500 μm to cm scale) were successfully transferred and the original donor Si wafer was clean enough for reuse after regular wafer cleaning (Fig. 1 *B* and *C*). Second, the Si NWs deposited by the contact-printing method (25) were highly aligned with uniform spacing before transfer (Fig. 1*C*, *Left*) and were fully embedded inside PDMS after transfer (Fig. 1*C*,

Author contributions: C.H.L., D.R.K., and X.Z. designed research, performed research, analyzed data, and wrote the paper.

The authors declare no conflict of interest.

*This Direct Submission article had a prearranged editor.

[1]To whom correspondence should be addressed. E-mail: xlzheng@stanford.edu.

www.pnas.org/cgi/doi/10.1073/pnas.0914031107

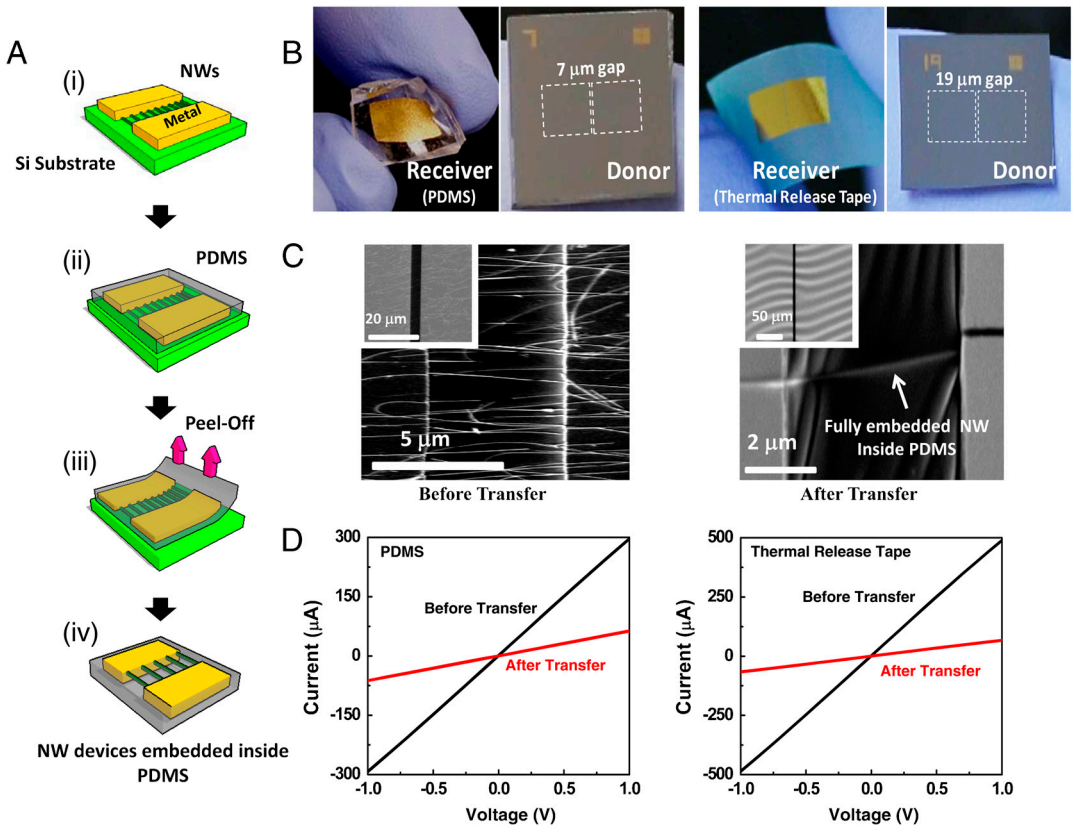

Fig. 1. Fabricating NW devices by using the STP method. (*A*) Illustration of the steps for the STP method on PDMS (Prefabricated NW devices → Deposition of liquid PDMS and curing → Peel off PDMS/NW devices → NW devices embedded inside PDMS). (*B*) Photographs of the NW devices on PDMS (*Left*) and a thermal release tape (*Right*), showing that all metal electrodes on the donor substrate were successfully transferred to the receiver substrate. The transferred NW devices show optical clarity and mechanical flexibility. (*C*) SEM images of a NW device before and after transfer to PDMS. The Si NWs deposited by the contact-printing method were well-aligned between two metal electrodes on the original Si wafer (*Left*) and were embedded inside PDMS after transfer (*Right*). (*D*) The *I–V* curves before and after transfer to PDMS (*Left*) and the thermal release tape (*Right*) remain linear although the current level decreases after the transfer.

Right), thereby enhancing the mechanical robustness of the NW devices. Finally, about 50–70% of the original devices were successfully transferred with retained linear current–voltage (*I–V*) curves (Fig. 1*D*), and the rest of the devices have either nonlinear *I–V* curves or no response. The device yield highly depends upon the number of NWs connecting the original device because the peel-off stress can break about 80–85% of NWs on the basis of the conductance reduction after transfer (Fig. 1*D*). Nevertheless, the transferred NW devices remain conductive, with linear *I–V* curves (Fig. 1*D*), so that they are still functional devices on PDMS and tapes. These results illustrate the potential of using the STP method to fabricate large-scale, well-defined NW devices on diverse flexible substrates.

The key factor for a successful STP method is to create large metal adhesion differences between the donor and the receiver substrates. Weak adhesion between the metal electrodes and the donor substrate facilitates a clean peel-off process (27, 28), so we choose metals such as Au and Pd, which adhere poorly to Si, as the bottom layer of the metal contact. Correspondingly, a strong adhesion between the metal electrodes and the receiver substrate is essential for reliable transfer and the robustness of the final devices. Although chemical or plasma treatments can enhance adhesion between Au or Pd films and polymers (20, 29), these treatments can change the surface chemistry of NWs and cause surface damage. Instead, we added a layer of Ti (5 nm) to the top of the metal contact during the metal evaporation step to enhance the adhesion between the metal electrodes and PDMS (20) while avoiding any damage to the NWs.

Importantly, the STP method has the potential to achieve stretchable metal interconnects for NW devices on PDMS. As shown in Fig. 2*A*, the initial flat metal electrodes become wave-like after transfer because they experience excessive stresses during the curing of PDMS (26, 30–32). The periodic wrinkles of the metal surface after transfer onto PDMS are clearly seen in Fig. 2*A*, and the wavy interconnect electrodes are essential for fabricating stretchable NW electronic systems for many applications, including NW tactile sensors for humanoid robots (33) and shape-conforming NW sensors. On the other hand, the metal surface transferred to tapes remains unwrinkled and smooth on the thermal release tape (Fig. 2*B*). Moreover, although we

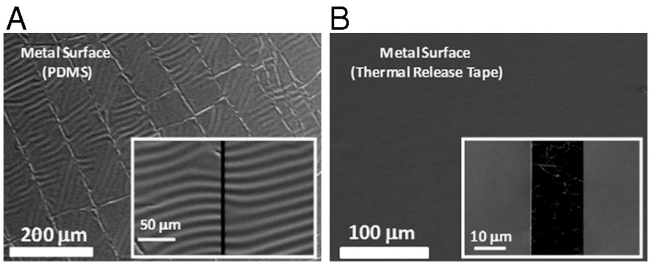

Fig. 2. SEM images of the transferred metal surfaces to PDMS (*Left*) and a thermal release tape (*Right*). (*A*) Metal surface becomes wrinkled with a sinusoidal wave-like pattern when it is transferred by PDMS because it experiences excessive stresses during the curing of PDMS. (*B*) Metal surface remains smooth when it is transferred to a thermal release tape. The insets show the enlarged images at the center position of two electrodes.

observed small cracks in a small area of the transferred metal surfaces because the excessive peel-off stresses, the metal surface transferred to tapes is, in general, uniform across the entire substrate, with at least 90% of the surface area being defect-free.

DTP Method for Fabricating NW Mesh Devices on Tapes. Fabricating NW mesh devices on tapes can be further simplified by using the DTP method. The DTP method transfers NWs and prepatterned electrodes from their respective donor substrates to the same tape receiver substrate in sequence, and its major steps are illustrated in Fig. 3*A*. First, Si NWs were grown on a growth substrate by using the Au-catalyzed vapor–liquid–solid mechanism (34, 35). Si NWs were subsequently etched by a buffered oxide etch (BOE, 20:1) to remove their surface native oxide in order to form good metal-silicon electrical contacts (Fig. 3*A*(*i*) (9). Second, an adhesive tape was gently applied to the top of the growth substrate and then peeled off by hand. As a result, many Si NWs were transferred onto the tape, forming an interconnected Si NW mesh network (Fig. 3*A*(*ii*), as shown in the left SEM image of Fig. 3*B*. Finally, the adhesive tape with the SiNW mesh was gently pressed against another Si donor wafer on which predefined metal electrodes had been patterned by photolithography. Peel-off of this adhesive tape resulted in the transfer of the metal electrodes, and these metal electrodes form direct contact with Si NW mesh on the tape (Fig. 3*A*(*iii*). As shown in the right SEM image of Fig. 3*B*, the final NW devices on the tape substrate consisted of NW meshes with metal contacts on two ends of Si NW mesh. Again, the metal surfaces are smooth, without wrinkles, as observed for the STP method. In addition, the density of the NW mesh can be increased further by the repetition of steps (*i*) and (*ii*) in Fig. 3*A*.

The DTP method is a general way to fabricate NW mesh devices on adhesive substrates. With this method, we have successfully fabricated NW mesh devices on blue wafer mount tapes, Kapton tapes (8), and thermal release tapes (Fig. 3*C*). Almost all the fabricated devices show *I*–*V* signals and about 30–40% of device have linear *I*–*V* curves, as shown in Fig. 3*D*, indicating that excellent ohmic contacts are formed between the NW mesh and metal electrodes with this simple pasting step. We believe that the strong adhesion between the metal electrodes and adhesive tape is responsible for the observed good quality of these contacts, which are found to be comparable to those made by the direct evaporation of metals on top of NWs. These NW mesh devices on tapes have two attractive and unique characteristics. First, they are transparent and flexible and can be pasted onto any flat or curved surface with the devices being protected by the tapes (Fig. 3*C*). Second, the NW mesh devices can be fabricated over large areas with controllable NW density.

MTP Method for Fabricating NW Mesh Devices on Diverse (*Flexible and Rigid*) Substrates. The MTP method, which is the third method we have developed, is the most versatile printing method and is able to fabricate NW mesh devices on diverse substrates including both rigid and flexible substrates. The important procedures of the MTP method are illustrated in Fig. 4*A*. First, a thermal release tape was pressed against a donor substrate carrying prefabricated metal electrodes and was then gently peeled off. As a result, the electrodes were cleanly transferred to the thermal release tape (Fig. 4*A*(*i*). Second, the thermal release tape carrying the electrodes was pressed down against various substrates, including Si wafers, tapes, and Petri dishes (Fig. 4*A*(*ii*). Then the whole device was heated at 90 °C for a few seconds to release the thermal release tape, allowing it to be peeled off easily, leaving only the metal electrodes on the target substrate (Fig. 4*A*(*iii*). Third, the BOE-etched Si NWs were transferred to adhesive tapes with controllable density by using the same procedure as that in the DTP method, as illustrated again in the right column of Fig. 4*A*. Finally, the tape with NW mesh was pasted onto the substrate with metal electrodes to complete the NW mesh devices (Fig. 4*A*(*iv*). Here the tape only partially covers the electrodes so that the exposed portions of the electrodes can be used for electrical connections.

The major advantage of the MTP method is that it can be used to fabricate NW mesh devices on any substrate with weak adhesive properties or even nonadhesive substrates, provided that

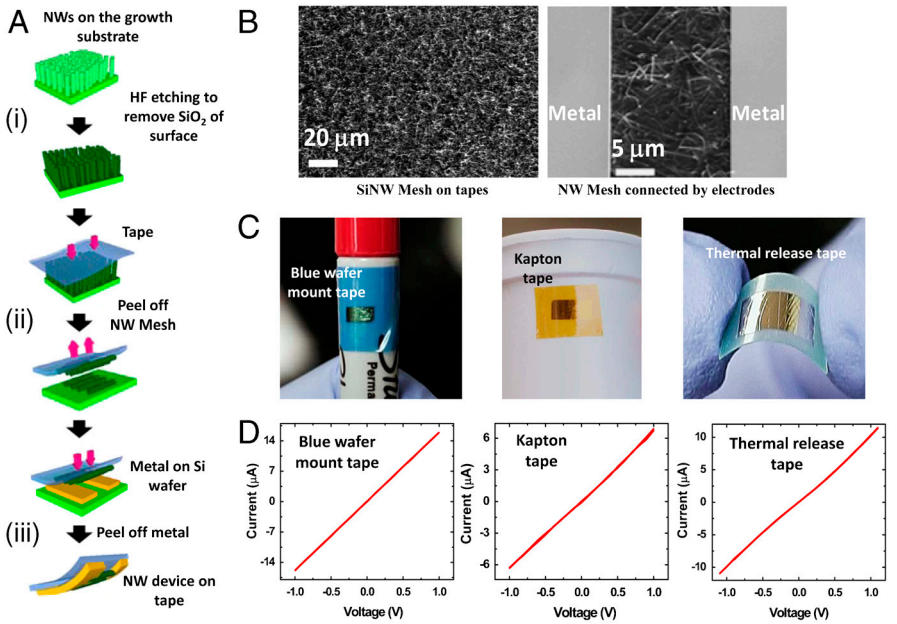

Fig. 3. Fabricating NW devices by using the DTP method. (*A*) Illustration of the steps for the DTP method (NWs on the growth substrate → HF etching to removethe native SiO_2 of NWs → Pressing down a tape to the NWs → Peel off the tape with NW mesh → Pressing down the tape/NW mesh to the prefabricated electrodes → 2nd Peel-off → NW device on the tape). (*B*) SEM images of Si NW mesh on the adhesive side of a tape (*Left*) and the transferred metal electrodes on top of the NW mesh on a thermal release tape (*Right*). (*C*) Photographs of the transferred NW mesh devices on a blue wafer mount tape (*Left*), a Kapton tape (*Middle*), and a thermal release tape (*Right*). All substrates have excellent mechanical flexibility. (*D*) The *I*–*V* curves of the final *p*-type Si NW mesh devices on the blue wafer mount tape (*Left*), the Kapton tape (*Middle*), and the thermal release tape (*Right*) are all linear indicating that the ohmic contacts were formed between the NW mesh and the metal electrodes.

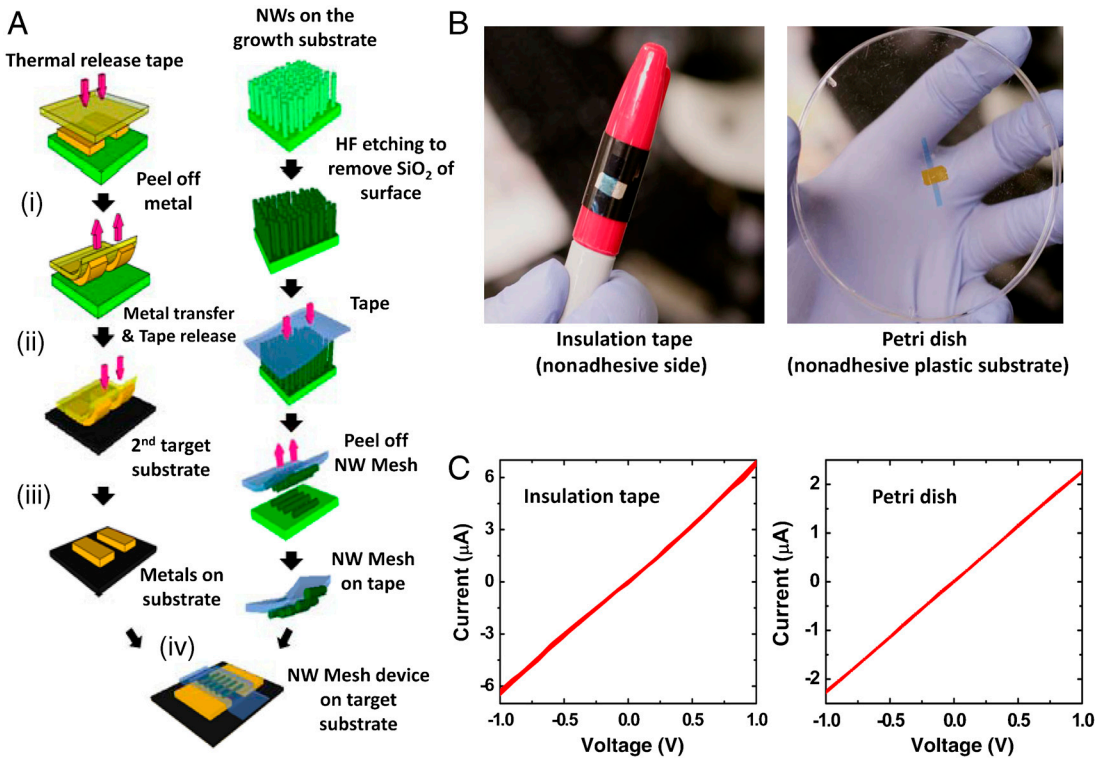

Fig. 4. Fabricating NW devices by using the MTP method. (*A*) Illustration of the steps for the MTP method (*1st column*: Pressing down a thermal release tape to the prefabricated electrodes → Peel off the thermal release tape with electrodes → Pressing down the thermal release tape/electrodes to a target substrate → The thermal release tape is thermally released at 90 °C; *2nd column*: NWs on the growth substrate → HF etching to remove the native SiO_2 of NWs → Pressing down a tape to the NWs → Peel off the tape with NW mesh → Assembling of the tape/NWs and the transferred electrodes). (*B*) Photographs of NW mesh devices fabricated by the MTP method on the nonadhesive side of an insulation tape (*Left*) and a Petri dish (*Right*). (*C*) The *I–V* curves of the *p*-type Si NW mesh devices fabricated on the insulation tape (*Left*) and the Petri dish (*Right*) are both linear.

their surfaces have sufficient roughness to hold the metal electrodes. For example, with the MTP method, we have successfully fabricated NW mesh devices on the nonadhesive side of an insulation tape and on a Petri dish, as shown in Fig. 4*B*, where the blue wafer mount tape attached on the NW mesh device was used to transfer and secure the Si NW meshes. We believe that metal electrodes are likely to be held on nonadhesive surfaces by van der Waals forces, because the MTP method does not work well for smooth substrates such as glasses and papers. Furthermore, similar to the DTP method, almost all the transferred NW mesh devices on the insulation tape and Petri dish show *I–V* signals and about 30–40% of device have linear *I–V* curves (Fig. 4*C*). These encouraging results suggest that the MTP method has great potential to be a simple and reliable method to fabricate NW mesh devices on diverse substrates.

Applications of NW Devices Fabricated by Transfer-Printing Methods. The three transfer-printing methods discussed above significantly broaden the types of substrates that NW devices can be fabricated on and, hence, will allow NW devices to be used for a wide range of applications such as strain/stress measurements in cell biology, biomedical devices, and piezotronic sensors (36, 37). To demonstrate these potentials, we have fabricated a piezoresistive sensor with *p*-type Si NWs (40 nm, 4,000:1) by the STP method on a flexible PDMS substrate (Fig. 5*A*). The sensing principle is based on the piezoresistive property of Si (37) whereby the electrical conductivity of Si NWs changes when Si NWs are deformed under applied stresses. To test this sensor, the electrical properties of the SiNW sensor were measured while mechanical strains were applied to the flexible sensor at room temperature (see *Materials and Methods*). Experimental results are shown in Fig. 5*B*, in which it can be clearly seen that the conductance of the Si NWs decreases under tension and increases under compression. This trend is consistent with the piezoresistive behavior of epitaxially grown *p*-type Si NWs tested by four-point bending experiments (37) and the piezoresistive behavior of bulk Si (38, 39). Importantly, the conductance of the Si NWs returned to its original value once the stress was released (Fig. 5*B*, *Inset*), confirming the robustness of NW devices fabricated by the STP method.

To further demonstrate the reliability of NW devices fabricated by the transfer-printing methods, we have transferred and printed a Si NW temperature sensor device on a SiO_2(600 nm)/Si wafer by using the MTP method. The sensing elements are 20 nm intrinsic Si NWs (i-Si NWs) grown by the vapor–liquid–solid mechanism (see *Materials and Methods*). The conductance of these i-Si NWs increases with increasing temperature as more charge carriers are thermally excited, thereby allowing the temperature to be measured. The conductance of the i-Si NWs was measured over a temperature range of 25–150 °C (see *Materials and Methods*), and the results are illustrated in Fig. 5*C*. It can be seen that the conductance of the i-Si NWs is higher at elevated temperatures, a result that is qualitatively consistent with similar measurements on bulk intrinsic Si (40, 41). Moreover, the *I–V* curves remain linear over the entire range of temperatures tested, providing further evidence for the excellent quality and robustness of NW devices fabricated by the transfer-printing methods.

It should be noted that, although poor metal and NW contact can also lead to the resistance change observed during bending and heating, it is unlikely to be the major reason here, because contact resistance change typically exhibits hysteresis and the *I–V* curves are unlikely to recover to the original ones after bending or heating, as observed here.

Conclusions

In summary, we have demonstrated three transfer-printing methods (STP, DTP, and MTP) to fabricate NW devices on flexible

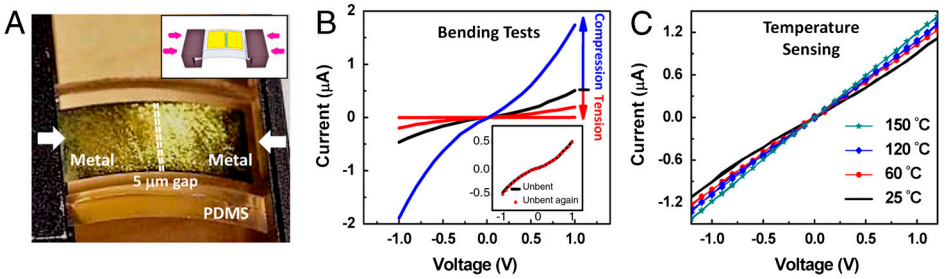

Fig. 5. Applications of Si NW devices fabricated by the transfer-printing methods. (*A*) Photograph and schematic figure (*Inset*) of experimental setup for testing the piezoresistive *p*-type Si NW sensor. The Si NW device was fabricated on PDMS by the STP method. (*B*) The conductance of the *p*-type Si NWs (40 nm, 4,000:1) increases under compressive stresses and decreases under tensile stresses. The inset shows that the *I–V* curve recovers to its original values when the stresses are released. (*C*) Temperature sensing with the *i*-type Si NW (20 nm) device fabricated by the MTP method. The conductance of the *i*-type Si NWs increases with increasing temperature.

and/or transparent substrates including PDMS, Petri dishes, and many types of adhesive tapes. NW devices fabricated by the transfer-printing methods exhibit several key features, including ohmic contacts between NWs and metal electrodes, controllable density of NWs per device, variable resolutions of electrode gaps from 3 up to 25 μm, and robustness against bending and heating. Moreover, NW devices fabricated by the transfer-printing methods are functional and reliable devices as demonstrated by our studies of flexible piezoresistive Si NW sensors on PDMS and Si NW temperature sensors. Nevertheless, there are still issues needing to be addressed for these transfer methods, such as improving the metal contact quality, increasing the device yield, exposing embedded NWs on PDMS for sensing applications, and enabling fabricating single NW devices or multilayered NW devices (e.g., field effect transistors) with controlled NW orientation. Finally, these transfer-printing methods can also be extended to pattern electrodes for organic electronics, reducing the need to protect the organic compounds during the fabrication process.

Materials and Methods

Synthesis of *p*- and *i*-Type Si NWs. Both *p*-type and *i*-type Si NWs were synthesized by chemical vapor deposition with 20- or 40-nm gold catalysts via the vapor–liquid–solid mechanism (34, 35). For the *p*-type Si NWs, the feeding ratio of Si:B was 4,000:1, and the growth condition was 440 °C, 40 Torr, 10 sccm of Ar, 2.5 sccm of SiH_4, and 3 sccm of 10,000:1 H_2 diluted B_2H_6. For the i-Si NWs, the growth condition was 485 °C, 40 Torr, and 50 sccm of SiH_4 (2% diluted in Ar).

Fabrication of NW Devices on the Donor Si Wafer. Devices were fabricated on degenerately doped silicon wafers with 600 nm thermally grown oxides. The *p*-type Si NWs (40 nm, 4,000:1) were deposited by the contact-printing method (25), which involves directional sliding of the Si NW growth substrate against the device substrate, resulting in the well-aligned NWs on the device substrate. The electrode patterns were defined by photolithography where the native oxide on NW under contact was etched in 20:1 BOE for 6 s, followed by metal deposition of Au/Ti or Pd/Ti (100 nm/5 nm) by an electron beam evaporator. The sacrificial photoresist layers were lifted off in acetone.

Characterization of *p*-Type Si NW Piezoresistive Sensor. The piezoresistive *p*-type Si NW sensor was fabricated by the STP method as shown in Fig. 1*A*. The mechanical manipulation of the NW devices embedded inside PDMS was realized by a micromanipulator (Melles Griot) loaded in a probe station (Signatone). While the micromanipulator applied tensile or compressive stresses to the NW devices, the conductance of the Si NWs was measured simultaneously in the probe station by using the measurement probes (XYZ-500; Quarter-Research) with the aid of a video microscope. Data were collected with a custom-programmed software routine (National Instruments LabVIEW).

Characterization of *i*-Type Si NW Temperature Sensor. The *i*-type NW temperature sensor was fabricated on a Si/SiO_2 wafer by the MTP method as shown in Fig. 4*A* (left column), except that the NWs were transferred to the wafer by the contact-printing method (25). For the temperature sensing measurement, a hot plate was installed in the chamber of a probe station and the assembled NW device was placed on the hot plate. The temperature was changed over a range of 25–150 °C, and the conductance of the Si NWs was measured simultaneously in the probe station by using the measurement probes.

ACKNOWLEDGMENTS. The authors thank Nitto Denko for the 3196 thermal release tapes and Pratap M. Rao for proofreading of the manuscript. D.R.K acknowledges support from the Link Foundation Energy Fellowship. X.L.Z. sincerely thanks the Defense Advanced Research Projects Agency/Young Faculty Award program and National Science Foundation under Award 0826003 for support of this work.

1. Il Park W, Zheng GF, Jiang XC, Tian BZ, Lieber CM (2008) Controlled synthesis of millimeter-long silicon nanowires with uniform electronic properties. *Nano Lett* 8(9):3004–3009.
2. Lu W, Lieber CM (2006) Semiconductor nanowires. *J Phys D Appl Phys* 39(21): R387–R406.
3. Huang Y, et al. (2001) Logic gates and computation from assembled nanowire building blocks. *Science* 294(5545):1313–1317.
4. Yan R, et al. (2009) Nanowire photonics. *Nat Photon* 3(10):569–576.
5. Zimmler MA, et al. (2008) Scalable fabrication of nanowire photonic and electronic circuits using spin-on glass. *Nano Lett* 8(6):1695–1699.
6. McAlpine MC, Friedman RS, Lieber CM (2005) High-performance nanowire electronics and photonics and nanoscale patterning on flexible plastic substrates. *Proc IEEE* 93(7):1357–1363.
7. McAlpine MC, Lieber CM (2004) High-performance nanowire electronics and photonics on glass and plastic substrates. *Abstr Pap Am Chem Soc* 227:236-PHYS.
8. Cohen-Karni T, Timko BP, Weiss LE, Lieber CM (2009) Flexible electrical recording from cells using nanowire transistor arrays. *Proc Natl Acad Sci USA* 106(18):7309–7313.
9. Patolsky F, Zheng GF, Lieber CM (2006) Fabrication of silicon nanowire devices for ultrasensitive, label-free, real-time detection of biological and chemical species. *Nat Protoc* 1(4):1711–1724.
10. Patolsky F, Zheng GF, Lieber CM (2006) Nanowire-based biosensors. *Anal Chem* 78(13):4260–4269.
11. Law M, Sirbuly DJ, Yang PD (2007) Chemical sensing with nanowires using electrical and optical detection. *Int J Nanotechnol* 4(3):252–262.
12. Kim DR, Lee CH, Zheng XL (2009) Probing flow velocity with silicon nanowire sensors. *Nano Lett* 9(5):1984–1988.
13. Kim DR, Zheng XL (2008) Numerical characterization and optimization of the microfluidics for nanowire biosensors. *Nano Lett* 8(10):3233–3237.
14. Lieber CM, Wang ZL (2007) Functional nanowires. *MRS Bull* 32(2):99–108.
15. Law M, Goldberger J, Yang PD (2004) Semiconductor nanowires and nanotubes. *Ann Rev Mater Res* 34:83–122.
16. Zhiyong F, et al. (2009) Toward the development of printable nanowire electronics and sensors. *Adv Funct Mater* 21(37):3730–3743.
17. Ju SY, et al. (2007) Fabrication of fully transparent nanowire transistors for transparent and flexible electronics. *Nat Nanotechnol* 2(6):378–384.
18. McAlpine MC, Ahmad H, Wang DW, Heath JR (2007) Highly ordered nanowire arrays on plastic substrates for ultrasensitive flexible chemical sensors. *Nat Mater* 6(5):379–384.
19. Zhao YZ, et al. (2009) Three dimensional metal pattern transfer for replica molded microstructures. *Appl Phys Lett* 94(2):023301–023303.
20. Loo YL, Willett RL, Baldwin KW, Rogers JA (2002) Additive, nanoscale patterning of metal films with a stamp and a surface chemistry mediated transfer process: Applications in plastic electronics. *Appl Phys Lett* 81(3):562–564.
21. Ahn JH, et al. (2006) Heterogeneous three-dimensional electronics by use of printed semiconductor nanomaterials. *Science* 314(5806):1754–1757.
22. Xinhong Y, Shunyang Y, Zhe W, Dongge M, Yanchun H (2006) Metal printing with modified polymer bonding lithography. *Appl Phys Lett* 88(26):263511–263517.
23. Lee K, et al. (2008) Nonaqueous nanoscale metal transfer by controlling the stickiness of organic film. *Langmuir* 24(16):8413–8416.

24. Thangawng AL, Ruoff RS, Swartz MA, Glucksberg MR (2007) An ultra-thin PDMS membrane as a bio/micro-nano interface: Fabrication and characterization. *Biomed Microdevices* 9(4):587–595.
25. Zhiyong F, et al. (2008) Wafer-scale assembly of highly ordered semiconductor nanowire arrays by contact printing. *Nano Lett* 8(1):20–25.
26. Yugang S, Won Mook C, Hanqing J, Huang YY, Rogers JA (2006) Controlled buckling of semiconductor nanoribbons for stretchable electronics. *Nat Nanotechnol* 1(3): 201–207.
27. Soo Young K, Kisoo K, Kihyon H, Jong-Lam L (2009) Investigation of metal peel-off technique for the fabrication of flexible organic light-emitting diodes. *J Electrochem Soc* 156(9):J253–257.
28. Kendall K (1971) Adhesion and surface energy of elastic solids. *J Phys D-Appl Phys* 4(8):1186–1195.
29. Keon Jae L, Fosser KA, Nuzzo RG (2005) Fabrication of stable metallic patterns embedded in poly(dimethylsiloxane) and model applications in non-planar electronic and lab-on-a-chip device patterning. *Adv Funct Mater* 15(4):557–566.
30. Stafford CM, et al. (2004) A buckling-based metrology for measuring the elastic moduli of polymeric thin films. *Nat Mater* 3(8):545–550.
31. Khang DY, Rogers JA, Lee HH (2009) Mechanical buckling: Mechanics, metrology, and stretchable electronics. *Adv Funct Mater* 19(10):1526–1536.
32. Lacour SP, Jones J, Wagner S, Li T, Suo ZG (2005) Stretchable interconnects for elastic electronic surfaces. *Proc IEEE* 93(8):1459–1467.
33. Kerpa O, Weiss K, Worn H (2003) Development of a flexible tactile sensor system for a humanoid robot. *Proceedings 2003 IEEE/RSJ International Conference on Intelligent Robots and Systems* (IEEE Robotics and Automation Society, Las Vegas, NV), pp 1–6.
34. Wagner RS, Ellis WC (1964) Vapor-liquid-solid mechanism of single crystal growth (new method growth catalysis from impurity whisker epitaxial + large crystals Si E). *Appl Phys Lett* 4(5):89–90.
35. Cui Y, Lauhon LJ, Gudiksen MS, Wang JF, Lieber CM (2001) Diameter-controlled synthesis of single-crystal silicon nanowires. *Appl Phys Lett* 78(15):2214–2216.
36. Zhou J, et al. (2008) Flexible piezotronic strain sensor. *Nano Lett* 8(9):3035–3040.
37. Rongrui H, Peidong Y (2006) Giant piezoresistance effect in silicon nanowires. *Nat Nanotechnol* 1(1):42–46.
38. Lenkkeri JT (1986) Nonlinear effects in the piezoresistivity of p-type silicon. *Phys Status Solidi B* 136(1):373–385.
39. Smith CS (1954) Piezoresistance effect in germanium and silicon. *Phys Rev* 94(1):42–49.
40. Premchand BBK (2005) Bulk silicon based temperature sensor. thesis (University of South Florida, Tampa, FL).
41. L Ni FD, Rogel R, Salaün AC, Pichon L (2009) *Fabrication and Electrical Characterization of Silicon Nanowires Based Resistors* (European Materials Research Society, Strasbourg, France).